

Effect of Airplane Wing Mass Distribution on Flutter Phenomena Mode

Dr. Muhammad. A. R Yass, Dr. Muhammad Kheiraldeen, Mohammed Wajeeh Hussien Almeen
Electromechanical Department, University of Technology, Iraq
Mechanical Department, Al Nahrain University, Iraq
Computer Science Department, Dijlah University College, Iraq
mohd.yass97@gmail.com, dr.mohammedaskar@yahoo.com, mohammed.alameen@duc.edu.iq

Article Info

Volume 83

Page Number: 3459 - 3470

Publication Issue:

March - April 2020

Article History

Article Received: 24 July 2019

Revised: 12 September 2019

Accepted: 15 February 2020

Publication: 22 March 2020

Abstract:

The paper studied and prediction the natural frequency and mod shapes for deflection, slop, shear and moment for four assumed cases for swept wing transport airplane with tow engine and different amount of fuel using Myklestad method which deal with transfer matrix technique for solving the mathematic modeling for these four cases. The maximum effect of the first mode deflection and slop on the tip of the wing (case one) and maximum effect of the second mode shear and moment on the mean root chord of the wing (case four) which were the most critical case.

Keyword: - Vibration, Elementary beam theory, Aero elasticity, Airplane wing structural characteristics

1. Introduction

The integration of flutter mode shapes of wings plays an important role and dominant effects on the airframe strength carried a transient aerodynamic load has a different peak value with unsymmetrical load distribution along the axes of symmetry during flight [1], any control system design for an airplane the response should be accurate enough to deal with motion [2].

However, the modern life desire required high rage and speedy airplane for that swept wing, high aspect ratio and fuselage fitness required.

All these parameters increase the aero elasticity of airplane and its effect becomes large issue to be considered for static and dynamic control system especially in dynamic case with rigid airplane [3]. The dynamic effects are especially important in the design of automatic control systems because structural modes may introduce instabilities that would not arise with a rigid airplane. Besides, the aerodynamic forces

and moments under unsteady flow, the prediction of natural frequencies and modes should be considered as a function of time [4].

Derivation of theoretical expression can be done by Rayleigh-Ritz method using vibration of small cantilever beam for determining natural vibration and frequency [5]. Although the frequency of airplane wing (swept, un swept) can't be found exactly in ideal case thus the approximation solution can be used such solution present torsional vibration and couple bending of no uniform mass distribution on swept wing on fuselage [6]. Myklestad and Prohl developed a tabular method to find the modes and natural frequencies of structures, such as an airplane wing. It is generally known as the Myklestad method uses the transfer matrix technique for this method [7].

2. Mathematical Modeling

2.1 Beam Assumption

The following assumptions were made

in the derivation of the present work:

- Beam Theory- Elementary beam theory is applicable; axial loads, shear deformation, and damping are neglected.
- Airplane wing Structural Representation-The airplane wing structural characteristics is simulated by a lumped masses and spring stiffness's.

2.2 Myklestad Method

Myklestad and Prohl developed a tabular method to find the natural frequencies and mode shapes of structures, such as an airplane wing (as a cantilevered beam) or flying bodies (as a free-free beam). It is generally known as the Myklestad method. We shall use the transfer matrix technique for this discussion.

Following the finite element approach, a structure or a beam can be divided into segments. A typical segment of a beam, as illustrated in Fig. 1, consists of a mass less span and a point mass. The field transfer matrix of the span describes the flexural properties of the segment; the point transfer matrix of the mass describes the inertial effect of the segment.

To describe the field transfer matrix, consider the free-body sketch of a uniform beam of length L in span n as shown in Fig. 1(a). For equilibrium,

$$\begin{matrix} V_n^L & V_{n-1}^L & & M_n^L & M_{n-1}^R \\ L_n & & V_n^R & & \end{matrix} \quad (1)$$

Where M and V moment and the shear force respectively. Referring to Fig. 1(a), the change in the slope

Φ of the span is due to moment M_n^L and the shear V_n^L

$$\Phi_n^L - \Phi_{n-1}^L = \left(\frac{L}{EI}\right)_n M_n^L + \left(\frac{L^2}{2EI}\right)_n V_n^L \quad (2)$$

Substituting M_n^L and V_n^L from Eq. (1) in (2) and

Rearranging, we get

$$\Phi_n^L = \Phi_{n-1}^R + \left(\frac{L}{EI}\right)_n M_n^L - \left(\frac{L^2}{2EI}\right)_n V_{n-1}^R \quad (3)$$

The change in the deflection Y of the span is

$$Y_n^L - Y_{n-1}^R = L_n \Phi_{n-1}^R + \left(\frac{L^2}{2EI}\right)_n L_n^R + \left(\frac{L^3}{3EI}\right)_n V_n^L \quad (4)$$

The first term on the right is the deflection due to the initial slope of the span, the second term due to the moment and the third term the shear force. The shear

Deformation of the beam is assumed negligible.

Substituting M_n^L and V_n^L from Eq. (1) in (4) and

Rearranging, we obtain

$$Y_n^L = Y_{n-1}^R + L_n \Phi_{n-1}^R + \left(\frac{L^2}{2EI}\right)_n M_{n-1}^R + \left(\frac{L^3}{6EI}\right)_n V_{n-1}^R \quad (5)$$

The field transfer matrix is obtained by writing Equation. (1),

$$\begin{bmatrix} Y \\ \Phi \\ M \\ V \end{bmatrix}_n^L = \begin{bmatrix} 1 & L & \frac{L^2}{2EI} & -\frac{L^3}{6EI} \\ 0 & 1 & \frac{L}{EI} & -\frac{L^2}{2EI} \\ 0 & 0 & 1 & -L \\ 0 & 0 & 0 & 1 \end{bmatrix} \begin{bmatrix} Y \\ \Phi \\ M \\ V \end{bmatrix}_{n-1}^R \quad (6)$$

To derive the point transfer matrix, consider the free-body sketch of m_n in Fig. 1(b). The D'Alembert's inertia loads are $-\omega^2 m_n Y_n^L$ and $\omega^2 J_n \phi_n^L$ where J_n is the mass moment of inertia of m_n about its axis normal to the (XY) plane. Neglecting the applied force P and the torque T, the equations for shear and moment are

are $-c\omega^2 m_n$ and

$$\begin{aligned} V_n^R &= V_n^L - \omega^2 m_n Y_n^L & \text{and} \\ M_n^R &= M_n^L - \omega^2 J_n \phi_n^L \end{aligned} \quad (7)$$

For rigid body motion of m_n , we have

$$\phi_n^L = \phi_n^R \quad \text{and} \quad Y_n^L = Y_n^R \quad (8)$$

The point transfer matrix is obtained from Equation. (7) and (8).

$$\begin{aligned} \begin{bmatrix} Y \\ \phi \\ M \\ V \end{bmatrix}_n^R &= \begin{bmatrix} 1 & 0 & 0 & 0 \\ 0 & 1 & 0 & 0 \\ 0 & -\omega^2 J & 1 & 0 \\ -\omega^2 m & 0 & 0 & 1 \end{bmatrix}_n \begin{bmatrix} Y \\ \phi \\ M \\ V \end{bmatrix}_{n-1}^R \end{aligned} \quad (9)$$

The transfer matrix for the segment n is obtained by substituting the state vector $\{Z\}_n^L$ from Eq. (6) in (9)

$$\begin{aligned} \begin{bmatrix} Y \\ \phi \\ M \\ V \end{bmatrix}_n^R &= \begin{bmatrix} 1 & 0 & 0 & 0 \\ 0 & 1 & 0 & 0 \\ 0 & -\omega^2 J & 1 & 0 \\ -\omega^2 m & 0 & 0 & 1 \end{bmatrix}_n \begin{bmatrix} 1 & L & \frac{L^2}{2EI} - \frac{L^3}{6EI} \\ 0 & 1 & \frac{L}{EI} - \frac{L^2}{2EI} \\ 0 & 0 & 1 & -L \\ 0 & 0 & 0 & 1 \end{bmatrix} \end{aligned}$$

$$\begin{bmatrix} Y \\ \phi \\ M \\ V \end{bmatrix}_n^L \quad (10)$$

$$\begin{aligned} \begin{bmatrix} Y \\ \phi \\ M \\ V \end{bmatrix}_n^R &= \begin{bmatrix} 1 & 0 & \frac{L^2}{2EI} & \frac{L^3}{6EI} \\ 0 & 1 & \frac{L}{EI} & -\frac{L^2}{2EI} \\ 0 & -\omega^2 J & 1 - \omega^2 J \frac{L}{EI} & -L + \omega^2 J \frac{L^2}{2EI} \\ -\omega^2 m & -\omega^2 mL & -\omega^2 m \frac{L^2}{2EI} & 1 + \omega^2 m \frac{L^3}{6EI} \end{bmatrix}_n \begin{bmatrix} Y \\ \phi \\ M \\ V \end{bmatrix}_{n-1}^L \end{aligned} \quad (11)$$

Hence the general theory from Eq. (11) is that the state vector $\{Z\}_n^R$ at the end of the ith segment is related to

$\{Z\}_{i-1}^R$ at the beginning of the ith segment by the transfer matrix T_i .

$$\{Z\}_i^R = T_i \{Z\}_{i-1}^R \quad (12)$$

Applying Eq. (12) for n segments, therefore, the state vector $\{Z\}_n^R$ and $\{Z\}_0^R$ at station 0 are related as

$$\{Z\}_n^R = T_n [T_{n-1} \dots T_2 T_1] \{Z\}_0^R \quad (13)$$

which is called the recurrence formula?

The common boundary conditions for the beam problem are listed in Table 1. For example, the deflection Y and the moment M at a simple support must be zero while the slope ϕ and the shear V are unknown and nonzero. At the beginning point or station 0 of a beam there are two nonzero boundary conditions, dictated by the type of

support. Similarly, there are two nonzero boundary conditions at the other end of the beam.

The procedure for a natural frequency calculation is to assume a frequency ω as in the Holzer method. The ω that satisfies simultaneously the boundary conditions at both ends of the beam is a natural frequency.

To demonstrate the procedure of calculation the natural frequency with applied boundary conditions, a cantilevered beam of two lumped masses (m_1 and m_2)

with uniform flexural stiffness EI as shown in Figure (2). The recurrence formulas for the computations are.

$$\begin{Bmatrix} z \end{Bmatrix}_1^R = T_1 \begin{Bmatrix} z \end{Bmatrix}_0^R \quad \text{and} \quad \begin{Bmatrix} z \end{Bmatrix}_2^R = T_2 T_1 \begin{Bmatrix} z \end{Bmatrix}_0^R \quad (14)$$

where

$$\begin{Bmatrix} z \end{Bmatrix}_0^R = \begin{Bmatrix} Y \\ \phi \\ M \\ V \end{Bmatrix}_0^R = \begin{Bmatrix} 0 \\ 0 \\ M_0 \\ V_0 \end{Bmatrix}$$

and M_0 and V_0 are the unknown moment and shear at the fixed end. Applying Eq. (11) for first and second segments Figure(3), we get

$$\begin{Bmatrix} z \end{Bmatrix}_2^R = T \begin{Bmatrix} z \end{Bmatrix}_0^R \quad ; \quad T = T_2 T_1$$

or,

$$\begin{Bmatrix} Y \\ \phi \\ M \\ V \end{Bmatrix}_2^R = \begin{bmatrix} T_{11} & T_{12} & T_{13} & T_{14} \\ T_{21} & T_{22} & T_{23} & T_{24} \\ T_{31} & T_{32} & T_{33} & T_{34} \\ T_{41} & T_{42} & T_{43} & T_{44} \end{bmatrix} \begin{Bmatrix} 0 \\ 0 \\ M_0 \\ V_0 \end{Bmatrix} \quad (15)$$

M_2^R and V_2^R must be zero at the free end of the beam, that is

$$M_2^R = 0 = T_{33}M_0 + T_{34}V_0$$

$$V_2^R = 0 = T_{43}M_0 + T_{44}V_0 \quad (16)$$

For a nontrivial solution of the simultaneous homogenous equations, the determinant of the coefficients of M_0 and V_0 must be vanish, that is,

$$\Delta(\omega) = \begin{vmatrix} T_{33} & T_{34} \\ T_{43} & T_{44} \end{vmatrix} = 0 \quad (17)$$

Therefore, the frequencies (ω_1 and ω_2) will be obtained from Eq. (17)

3. Results Discussions

Myklestad-Prohl methods with a transfer matrix technique are illustrated in this project to estimate the flutter mode and shape six unequal division of semis pan wing with middle station point and some station could be chosen for accuracy desired. The space between stations it gives the number of station, and the first station touch the wing root or fuselage wing intersection, so fuselage force act at station 0 .other five stations locate at mass location or point of average mass distribution. Station five always at point close to wing tip and total mass distribution assumed to be constructed at station points. In this case the wing assumed to be beam subjected to six lad points and assumed linear moment behavior between stations. The physical characteristics for the airplane wing platform with the material used are listed in Table 1 [8]. The moment of inertia of airfoil cross -section about chord plane can be computed.

$$K_1 C_{\text{section}}^4 \left(\frac{t}{c}\right)^3 (m)^4$$

Where

t = airfoil thickness

$K1 = 0.0377$ for NASA 65A0xx

$$C_{\text{section}} = C_{\text{Tip}} + (S - y) \left(\frac{\tan LE}{\tan TE} - 1 \right) I$$

The variation of structural characteristics across the semi span of the wing i. e the variation of bending moment of inertia by using Eq. (18) with thickness ratio (t/c) equal 12%, bending rigidity that can be obtained by multiplying the results of Eq. (18) by the modulus of elasticity of Dura Aluminum alloy (it is assumed that the variation of EI is linear between each station) and the wing structural mass are presented in Figs. 4 and 5 respectively. Table 3 shows the wing structural data such as the lengths between each station and the station concentrated masses.

In the present work, four case studies are considered. The mass effects of engines airplane with the amount of fuel are shown in Table 4. One engine with half fuel is used in case one while the same engines with full fuel are considered in case two. Cases three and four, we took two engines with half and full fuel respectively.

The natural frequencies of the airplane wing for the four cases are presented in Table 5. It can be seen that case four have a smaller frequency for ail modes than other cases due to higher masses of engine and fuel. Figs. 6 and 7 show the first and second mode shapes in deflection (Y). As it illustrates in fig.6 that the deflection is zero at the root and increased gradually to maximum value at tip. Also, we observed that the case four have minimum value in deflection from other cases due to higher masses. For the second mode in deflection (see Fig. 7), all cases began from zero and

reaches maximum positive values for case one and two due to lower masses than others. At the wing tip, cases two and four have maximum negative values. Figs. 8 and 9 shows the first and second mode shapes in slope (ϕ). Fig.8 shows that the zero is zero at the root and increased gradually to maximum value at tip. Case four have a minimum value in slope from other cases. For the second mode in slope (see Fig. 9), all cases began from zero and reaches maximum positive values for case one and two. At the wing tip, case two has maximum negative value. Figs. 10, 11, 12 and 13 shows the first and second mode shapes in moment (M) and shear (V). Figs.10 and 12 shows that the moment and shear for all cases began with maximum positive values at the wing root and then decreased gradually until wing tip, they reach to zero (behavior of cantilever beam). Similarly, for the second mode (see Figs. 11 and 13), it began from maximum positive values, then reaches to maximum negative values (case four) at the middle of the wing semi span, after that they goes to zero.

4. Conclusions

For preliminary design, this method can be considered successful and used estimate the free vibration characteristics of any model with any type of constraints in the aero elastic solution of the flying bodies.

It can be that the maximum effect of first mode deflection and slope on the tip of wing and maximum effect of the first mode shear and moment on the root of wing (cantilever behavior), case one most critical case.

The maximum effect of second mode shear and moment on mean root of the wing and case four is more critical case

but for second mode deflection and slope, case two is most critical case (weight distribution).

Table 1. the common boundary condition of the beam

Boundary Condition	Deflection Y	Slope ϕ	Moment M	Shear V
SIMPLY SUPPORT	0	ϕ	0	
FREE	Y	ϕ	0	

Table 2. Physical Characteristics for Example Airplane

Wing Semi Span (m)	14.224
Root Chord (m)	3.91160090
Tip chord (m)	1.49031960
Wing Aspect Ratio	10.53
Wing Taper Ratio	0.381
Leading Edge Angle (deg)	35.0
Trailing Edge Angle (deg)	62.077
Airfoil Section	65A012
Thickness Ration (t/c)	12%
Wing Material Aluminum	Modulus of Elasticity $E = 6.870 * 10^9 \text{ N/m}^2$

Table 3. Airplane Wing Model-Structural Data

Stations	L (m)	EI (N.m ²)	m (kg)
0	1.28016	83307005.13	4846.05
1	2.56032	50416048.22	2727.0-1363.8
2	2.41808	29371501.12	322.425-644.8
3	2.27584	16359021.97	171.9
4	2.27584	8239871.71	90.45
5	2.27584	3599423.73	53.1

Table 4. Cases Study

Case Number	Specifications
Case 1	One Engine (1363.5 kg) + Fuel (322.425 kg)
Case 2	One Engine (1363.5 kg) + Fuel (644.85 kg)
Case 3	Two Engines (2727 kg) + Fuel (322.425 kg)
Case 4	Two Engines (2727 kg) + Fuel (644.85 kg)

Table 5. Airplane Wing Natural Frequencies

Case Number	Natural Frequency (rad / sec)					
	ω_1	ω_2	ω_3	ω_4	ω_5	ω_6
Case	17.81	52.01	111.7	208.3	271.7	410.2
Case	16.86	47.65	111.0	187.7	264.7	379.6
Case	17.23	44.50	101.7	208.2	258.3	405.2
Case	16.34	42.48	98.19	187.3	250.3	376.1

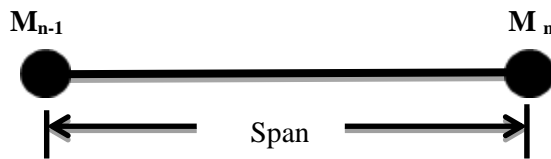


Figure (1) Free Body Sketch of m_n

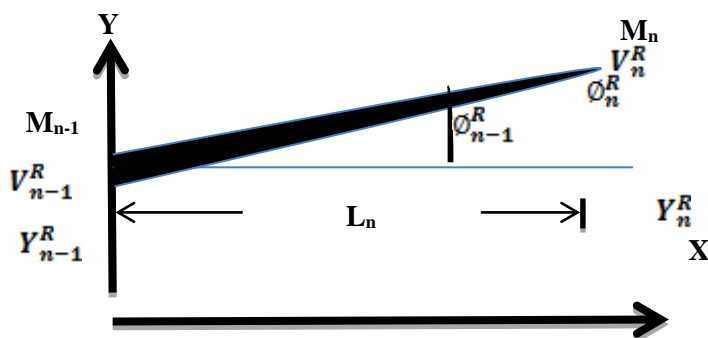


Figure (2) Cantilevered Beam of Two Lumped Mass

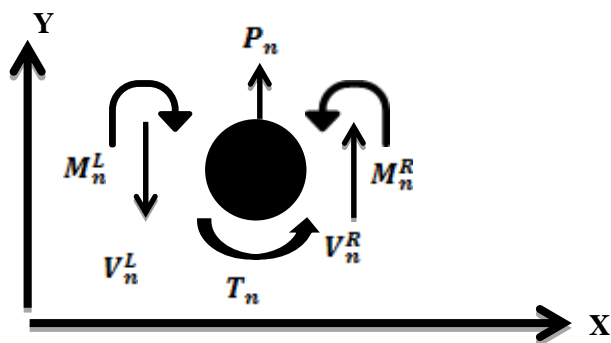


Figure (3) Derivation of transfer Matrix of a Beam

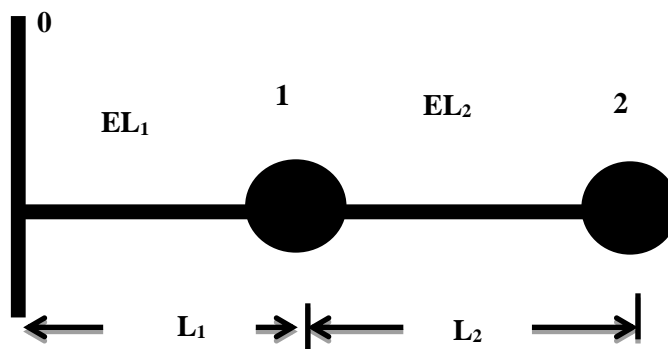


Figure (4) Lumped Mass Representation of a Beam

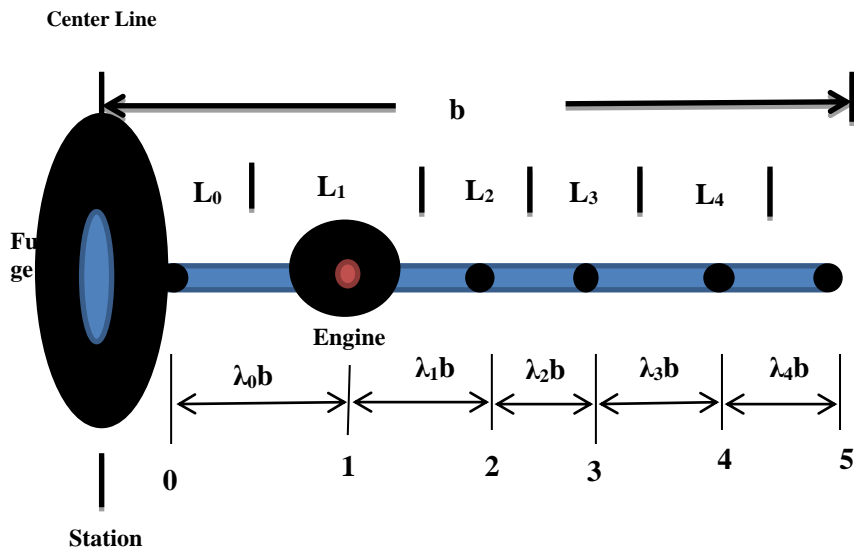


Figure (5) Division of Wing into Sections

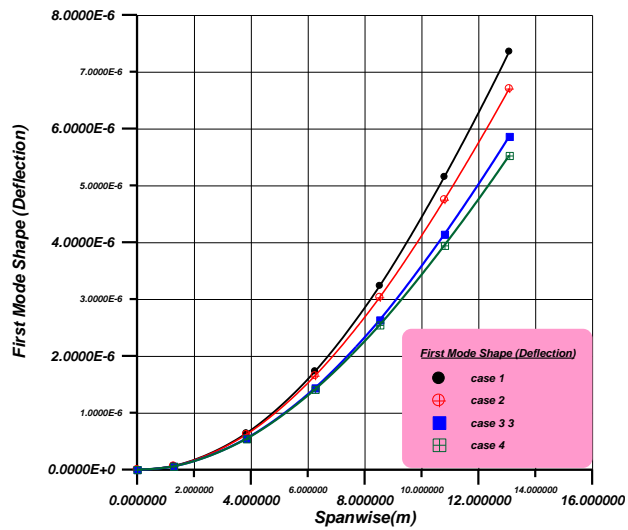


Figure (6) first mode shape (deflection)

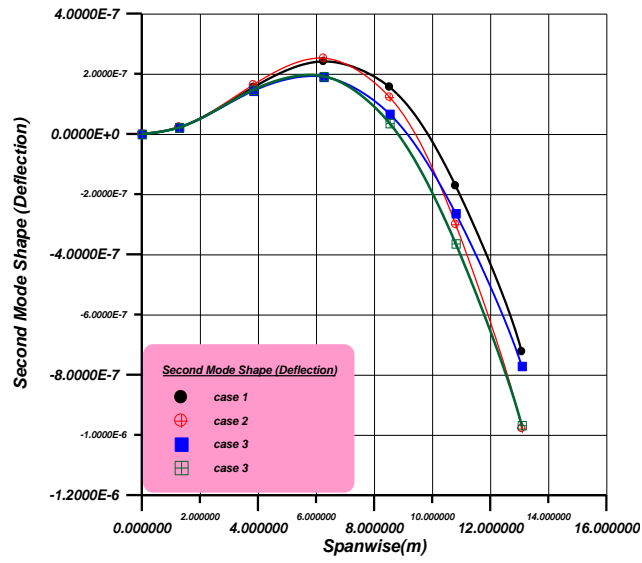


Figure (7) second mode shape (deflection)

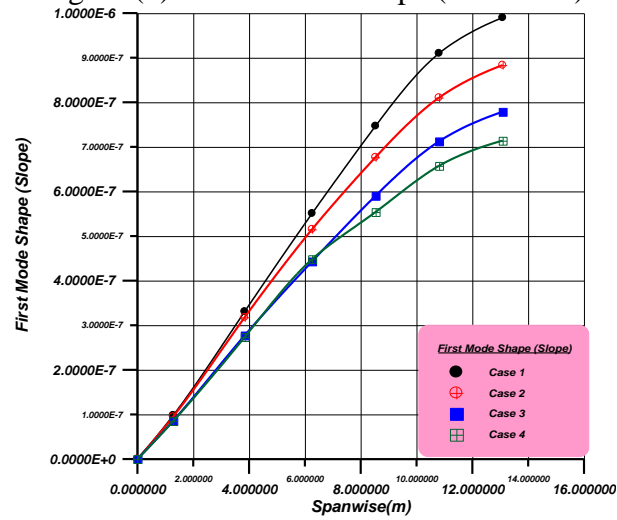


Figure (8) first mode shape (Slope)

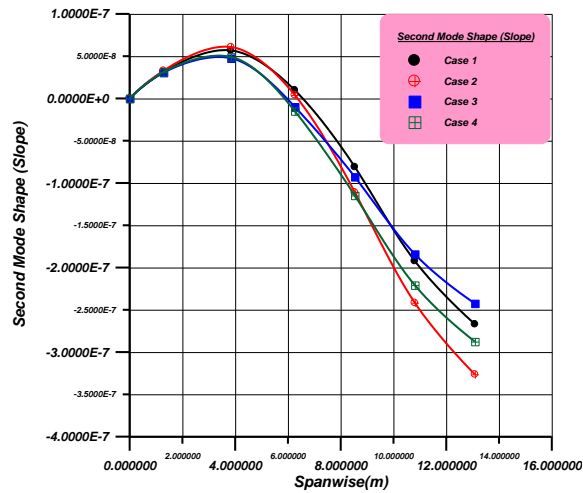


Figure (9) Second Mode Shape (Slope)

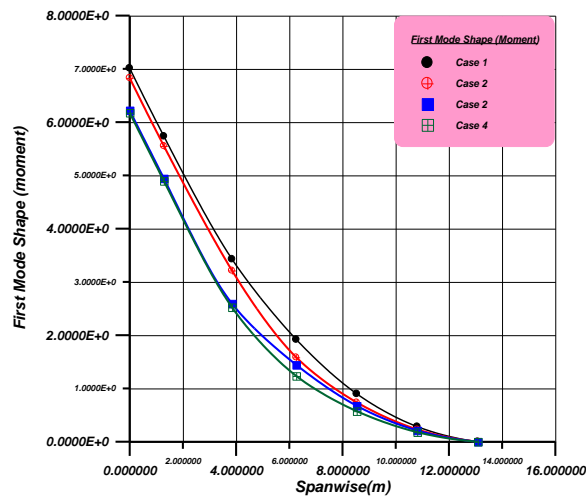


Figure (10) first mode shape (Moment)

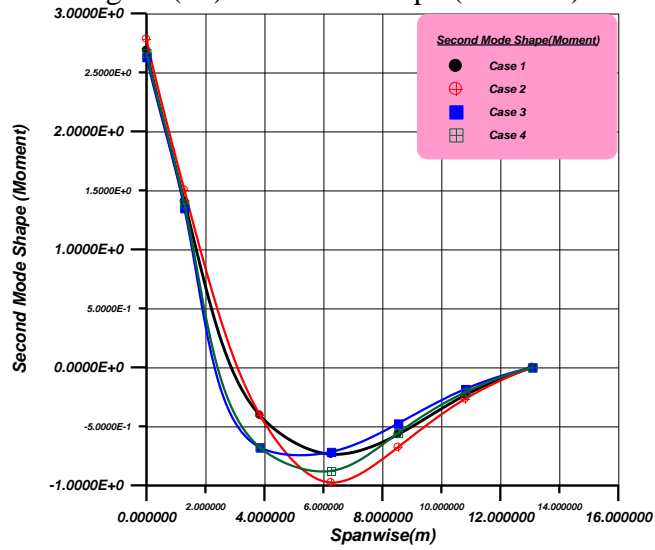


Figure (11) second mode shape

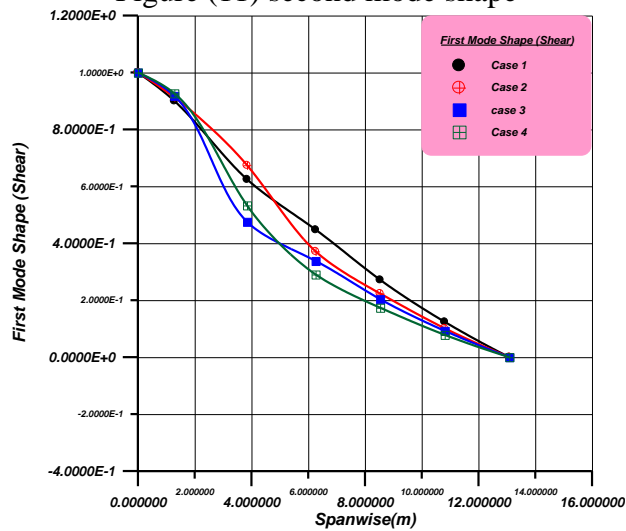


Figure (12) first mode shape (Shear)

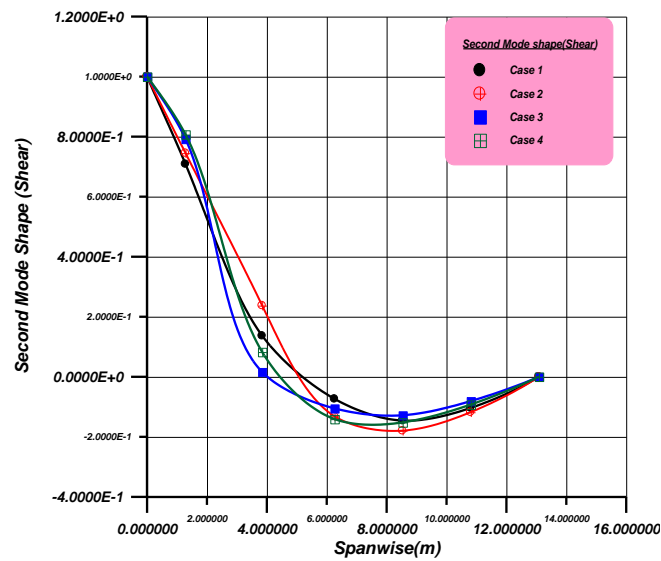


Figure (13) second mode shape (Shear)

5. List of Symbols

Symbol	definition	units
C_{section}	Chord Section	M
C_{Root}	Wing Root Chord	M
C_{Tip}	Wing Tip Chord	M
E	Modulus of Elasticity	N/m^2
I	Bending Moment of Inertia	M^4
J	Rotary Moment of Inertia	N.m.sec^2
L	Length between Lamped Mass	M
LE	Wing Leading Edge Angle	Degree
M	Bending Moment	N.m
V	Shear Moment	N
S	Wing Semi Span	M
TE	Wing Trailing Edge Angle	Degree
Y	Deflection(1 st Mode Shape)	-----
EL	Bending Rigidity	N.m^2
\emptyset	Slope(2 nd Mode Shape)	-----
ω	Natural Frequency	Rad/sec
T	Natural Matrix	-----
$\{Z\}$	State vector	-----

References

[1] Björn Persson, 2010, “Aeroelastic tailoring of a sailplane wing”, KTH – Royal Institute of Technology SE 100 44

Published by: The Mattingley Publishing Co., Inc.

Stockholm, Sweden.

[2] Rajeswari V. and Padma Suresh L., September 2015, “Design and Control of Lateral Axis of Aircraft using Sliding Mode Control Methodology”, Indian

- Journal of Science and Technology, Vol 8(24), IPL0386.
- [3] Kamlesh Purohit and Manish Bhandari, 2013," Determination of Natural Frequency of Airfoil Section Blades Using Finite Element Approach, Study of Effect of Aspect Ratio and Thickness on Natural Frequency", Engineering journal, Volume 17 Issue 2.
- [4] Burnett E., Atkinson C., Beranek J., Sibbitt B., Holm-Hansen B. and Nicolai L. 2010, "Simulation model for flight control development with flight test correlation," AIAA Modeling and Simulation Technologies Conference, Toronto, Canada, pp. 7780-7794.
- [5] Henry A. Cole, Jr., Stuart C. Brown, and Euclid C. Holliman, 1955, "The effects of flexibility on the longitudinal and lateral", NASA RM A55D14, Washington.
- [6] Carnegie W., 1962, "Vibration of pre twisted cantilever blades: An additional effect of torsion," ASME J. of Applied Mechanics, vol. 176, pp. 315-319.
- [7] Myklestad 1945 selected to determine the bending-torsion modes of beams (N. O. Myklestad, 1945, "New method of calculating natural modes of coupled bending- torsion vibration of beams," Transaction of the ASME, vol. 67, pp. 61-67.
- [8] John C. Houbolt, January 19, 1950;' A Recurrence Matrix Solution for the Dynamic Response of Aircraft in Gusts"; NACA Report No. 1010.
- [9] Kurt Strass H. and Emily W. Stephens, 1953;' An Engineering Method for the Determination of Aeroelastic Effects upon the Rolling Effectiveness of Ailerons on Swept Wings'; NACA RM L53H14.